New constitutive models for the finite deformation of isotropic compressible elastomers

Afshin Anssari-Benam[1] and Cornelius O. Horgan[2,*]

[1] Cardiovascular Engineering Research Lab (CERL),
School of Mechanical and Design Engineering,
University of Portsmouth,
Anglesea Road,
Portsmouth PO1 3DJ
United Kingdom

[2] School of Engineering and Applied Science,
University of Virginia,
Charlottesville,
VA 22904
USA

[*] Address for correspondence: Cornelius O. Horgan,
School of Engineering and Applied Science,
University of Virginia,
Charlottesville,
VA 22904
USA

Tel: 434-987-1937
ORCID: 0000-0003-0457-0732

E-mail: coh8p@virginia.edu

Abstract

The application of a new family of strain energy functions to modelling the finite deformation of isotropic *compressible* elastomers, including polymeric foams and (hydro)gels, is presented in this paper. The proposed family of models is developed from a *parent* incompressible strain energy function, customised to the *compressible* case via an additive split of *deviatoric* and *volumetric* contributions. With a minimum of four and maximum of five parameters, the developed models are shown to be compatible with the empirical deformation kinematics of *slight* compressibility (or almost incompressibility) and provide favourable fits to the extant deformation datasets by simultaneous fitting to uniaxial, biaxial and/or simple shear deformations. Some intricate behaviours such as the shear-softening of polystyrene foams and the ensuing instability under simple shearing, as well as the simple tension of alginate-based hydrogels under extremely high levels of stretch are also successfully modelled. Given the versatility of the proposed family of models in terms of their relatively low number of model parameters, their capability to predict a wide range of deformation behaviours for a wide range of elastomers (from foams to gels), and the robustness of the provided fits, the advantages of the considered models over the existing models of the same class in the literature is demonstrated.

Keywords: Polymeric foams, hydrogels, compressibility, finite deformation, modelling, strain energy function.

New constitutive models for the finite deformation of isotropic compressible elastomers

1. Introduction

While the theory of nonlinear elasticity for incompressible hyperelastic materials has been successfully applied to modelling the mechanical behaviour of rubbers, it is recognised that most rubber-like materials are indeed *compressible* in practice. Compressibility effects may reflect themselves to a lower degree in the mechanical behaviour of natural rubbers, e.g., vulcanised rubbers and pure gum have been reported to only experience a volume change of 1% and 2%, respectively, under simple tension of up to 700% elongation (see, e.g., Gent and Lindley, 1959; Holt and McPherson, 1936), and even lower (in order of 0.01%) under other types of deformation (Ogden, 1976). However, for some polymeric elastomers such as polyurethane (foams) and biopolymeric (hydro)gels, which are of concern in this work, the degree of compressibility is significantly higher; see, e.g., the classical works of Blatz and Ko (1962), Beatty and Stalnaker (1986), and Urayama et al. (1993). It may still be tempting to use incompressible models for these elastomers; see, e.g., a most recent review by Ding et al. (2021) where the performance of incompressible strain energy functions in application to polyurethane foams has been considered and evaluated. However, for a more robust modelling and characterisation of the mechanical behaviour of polymeric foams and gels, the *compressible* form of a strain energy function must be considered.

In addition to the experimental evidence, consideration of compressibility is also expedient from the point of view of computational simulation and Finite Element (FE) analysis. Enforcing full incompressibility in computational and FE simulations causes numerical difficulties and instabilities. Therefore, as a mitigating strategy, the mechanical behaviour of materials that are considered to be incompressible, such as soft tissues for example, are often computationally simulated by using a (slightly) *compressible* form of a strain energy function W, where the compressible (or hydrostatic) term W_{Vol} is considered as an additive term to the *deviatoric* W_{Dev} part of W; see, e.g., the recent papers by Li et al. (2018), Li and Holzapfel (2019) and Gültekin et al. (2019), *inter alia*, where W_{Vol} serves as a penalty function. Therefore, compressible forms of the strain energy function W play a key role in both accurate characterisation and computational simulation of the mechanical behaviour of rubber-like materials.

The aforementioned additive split of the strain energy function W into a *deviatoric* W_{Dev} and a *volumetric* W_{Vol} contribution is indeed a customary method for constructing a compressible form of W. The *deviatoric* part W_{Dev} is considered not to contribute to the change of volume that accompanies a deformation, which is instead solely accounted for via the *volumetric* part W_{Vol}. To this end, many mathematical forms of $W_{Vol}(J)$, where $J = \lambda_1\lambda_2\lambda_3$ and λ_i are the principal stretches, have been proposed – see Table 1 for a summary of specific functional forms of $W_{Vol}(J)$, and the works of Bischoff et al. (2001) and Horgan and Saccomandi (2004) for a detailed account of various W_{Vol} functions in the literature.

Table 1 – Some forms of $W_{Vol}(J)$ frequently used in the literature.

Proposed by	$W_{Vol}(J)$	Notes
Flory (1961)	$\beta_1 \ln J + \beta_2(\ln J)^2 + \beta_3(J^2 - 1)$	β_i are phenomenological parameters.
Blatz and Ko (1962)	$J - \ln J - 1$	A special case of $W_{Vol}(J)$ in Ogden (1972; 1976) with $\beta = -K = -1$.
Valanis and Landel (1967)	$\frac{K}{2}(\ln J)^2$	K is related to the bulk modulus.
Ogden (1972; 1976)	$\frac{K}{\beta^2}\left(\beta \ln J + J^{-\beta} - 1\right)$	K is related to the bulk modulus and β is a phenomenological parameter.
Sussman and Bathe (1987)	$K(J-1)^2$	Both functions are a special case of $W_{Vol}(J) = K[\beta_1(J-1)^2 + \beta_2(\ln J)^2]$, with $\beta_1 = 1$ and $\beta_2 = 0$ (Sussman and Bathe, 1987) and $\beta_1 = \beta_2 = 1$ (Simo and Taylor, 1982).
Simo and Taylor (1982)	$K[(J-1)^2 + (\ln J)^2]$	
Bischoff et al. (2001)	$\frac{K}{\beta^2}\{\cosh[\beta(J-1)] - 1\}$	K is related to the bulk modulus and β is a phenomenological parameter.

Depending on the empirical choice of the functional form of W_{Vol}, therefore, at least one but potentially more model parameters are added to the strain energy function $W(= W_{Dev} + W_{Vol})$. Accordingly, the well-known reservations for choosing an incompressible strain energy function also extend to, and are exacerbated when, choosing a compressible form of W. First, as stipulated by Yeoh (1997), the unwarranted extra model parameters in a strain energy function W, beyond what should be constitutively prescribed for the subject material, only leads to a model that fits better the experimental errors. This, consequently, leads to a strain energy function that is unstable; i.e., produces unrealistic behaviours outside the range of the experimental data (Yeoh, 1997). Second, as detailed by Ogden et al. (2004), an excessive

number of model parameters in W gives rise to issues surrounding the uniqueness of the optimal fit and thereby finding the optimal values of the model parameters. Both of the foregoing undesirable effects inherently pose a higher risk in modelling the compressible behaviour compared with the incompressible case, due to the unavoidable additional *volumetric* part in the strain energy function W. Therefore, for a robust modelling of the mechanical behaviour of a compressible elastomer, ideally one must seek a strain energy function W with minimum number of constitutive parameters.

Another challenge in modelling the behaviour of compressible materials, which is also applicable to the incompressible case, is calibrating the strain energy function W using datasets from multiple deformation modes. As demonstrated by Anssari-Benam and Bucchi (2021), fitting a model to only one deformation mode (say uniaxial tension, or biaxial loading or pure shear etc) may not lead to the *global* minimum of the residual function, which instead may be achieved by simultaneous fitting of the model to multiaxial data. The implication of this finding is that the *optimal* set of model parameter values are likely best found via simultaneous fitting of the model to the various deformation datasets of a specimen. In the case of polyurethane foams, for example, a recent study by Yan et al. (2021) has highlighted the modelling problems which may arise on using the Ogden hyperfoam model (Hill, 1979) in conjunction with only the simple shear data and has alternatively suggested strategies involving various datasets for a more robust calibration of the model. See also Anssari-Benam and Horgan (2021) for intricacies of modelling the simple shear deformation. Currently, the performance of the many of the existing models in the literature under simultaneous application to various deformation datasets obtained from polymeric foams and gels remains unclear, as most studies (due to difficulties in performing multiaxial mechanical tests on foams and gels) mainly focus on simple tension and/or compression behaviour. A robust strain energy function W for application to the deformation of polyurethane foams and hydrogels, however, must prove capable of adequately capturing various deformation behaviours of a specimen *via a single set of model parameter values*.

An additional consideration for choosing a compressible form of W is that it ideally has to be compatible with the whole range of compressibility behaviour, including *slight* compressibility (or almost incompressibility). Through the work of Beatty and Stalnaker (1986), it has been found that for a large class of almost incompressible rubbers, there is a power-law kinematic

relationship between the stretch in the direction of the applied force, and the two stretches perpendicular to this direction. The extensive work of Horgan and Murphy (2007a; 2007b; 2009a; 2009b; 2009c; 2009d), has established that many of the commonly used constitutive models in the literature do not capture this effect. A robust strain energy function for application to compressible materials, therefore, most possess the generic ability of capturing the slight compressibility effects too.

In view of the challenges in modelling the compressible behaviour of elastomers outlined in the foregoing, the aim of this manuscript is to present a new family of strain energy functions W that overcome these difficulties, resulting in a robust application to modelling the mechanical behaviour of compressible elastomers. The proposed family of models are based on a three-parameter *parent* generalised neo-Hookean W function developed by Anssari-Benam (2021), successfully applied to modelling the finite deformation of incompressible unfilled natural and filled rubbers, as well as silicone samples (see Anssari-Benam and Horgan, 2022b). A model of this family with an adjunct I_2 term (four parameters) will also be considered. The compressible forms of the models (see Eq. (12)), are then applied to extant experimental datasets pertaining to polyurethane foams and biopolymeric hydrogels, as archetypal examples of compressible rubber-like materials, via simultaneous fitting to the various considered deformation modes of each specimen. It will be shown that by possessing a low number of model parameters (a minimum of three to a maximum of five), this family of models are compatible with slight compressibility effects and favourably capture various deformations of the compressible elastomers with a single set of model parameter values. In Section 2 we present the formulations of the new models as well as compatibility with slight compressibility effects. The application of the models to the experimental data is made in Section 3, where the favourable modelling results are presented and discussed. Concluding remarks are given in Section 4.

2. A family of isotropic compressible models

A customary method to formulate a viable compressible form of the strain energy function W is to consider an additive volumetric part to a basic incompressible strain-energy function, in such a way to decompose the pure *deviatoric* contribution from the pure *volumetric* part of the deformation. See, e.g., Horgan and Saccomandi (2004) for more details and an overview

of different methods. In this method, the pure *deviatoric* part of the deformation is expressed by the modified principal stretches $\bar{\lambda}_i$, defined as (see, e.g., Ogden, 1976):

$$\bar{\lambda}_i = \lambda_i J^{-\frac{1}{3}}, \tag{1}$$

where:

$$J = \lambda_1\lambda_2\lambda_3 = \sqrt{I_3}, \tag{2}$$

and λ_i are the principal stretches. Since $\bar{\lambda}_1\bar{\lambda}_2\bar{\lambda}_3 = 1$, a deformation described by the modified principal stretches $\bar{\lambda}_i$ is isochoric. The *deviatoric* invariants $\bar{I}_1$ and $\bar{I}_2$ therefore immediately follow as:

$$\begin{cases} \bar{I}_1 = \bar{\lambda}_1{}^2 + \bar{\lambda}_2{}^2 + \bar{\lambda}_3{}^2 = J^{-\frac{2}{3}}(\lambda_1^2 + \lambda_1^2 + \lambda_1^2) = J^{-\frac{2}{3}} I_1, \\ \bar{I}_2 = \left(\bar{\lambda}_1\bar{\lambda}_2\right)^2 + \left(\bar{\lambda}_2\bar{\lambda}_3\right)^2 + \left(\bar{\lambda}_1\bar{\lambda}_3\right)^2 = J^{-\frac{4}{3}}(\lambda_1^2\lambda_2^2 + \lambda_2^2\lambda_3^2 + \lambda_1^2\lambda_3^2) = J^{-\frac{4}{3}} I_2, \end{cases} \tag{3}$$

where I_i are the usual principal invariants of the left Cauchy-Green deformation tensor $\mathbf{B}(= \mathbf{F}\mathbf{F}^{\mathrm{T}})$. Therefore, the general form of a compressible strain energy function W is expressed as:

$$W = W_{Dev}(\bar{I}_1, \bar{I}_2) + W_{Vol}(J). \tag{4}$$

Note that J, as given by Eq. (2), characterises the ratio of change in volume $J = V/V_0$.

For the *deviatoric* part W_{Dev}, we consider a three-parameter incompressible model recently devised by Anssari-Benam (2021), with the following functional form:

$$W_{Inc} = \frac{3(n-1)}{2n}\mu N\left[\frac{1}{3N(n-1)}(I_1 - 3) - \ln\left(\frac{I_1 - 3N}{3 - 3N}\right)\right], \tag{5}$$

where the subscript '*Inc*' denotes the incompressible form, and μ, N and n are model parameters. The parameter μ in the model is related to the infinitesimal shear modulus μ_0 via:

$$\mu_0 = 2\left(\frac{\partial W}{\partial I_1}\right)_{I_1=3} \Rightarrow \mu_0 = \frac{1}{n}\mu\frac{1-nN}{1-N} \Rightarrow \mu = \mu_0\frac{n(1-N)}{1-nN}. \tag{6}$$

The model in Eq. (5) is therefore subjected to the following rational constraints:

$$\mu_0 > 0 \quad , \quad \frac{I_1 - 3N}{3 - 3N} > 0. \tag{7}$$

It follows that, as analysed at length by Anssari-Benam and Horgan (2021; 2022b), for these constraints to hold true and the $\ln(\blacksquare)$ function to be well-defined, we require N to be a real-valued parameter and $n \in \mathbb{R}^{+}$. The model in Eq. (5) has been successfully applied to various deformation modes of incompressible filled and unfilled rubbers (Anssari-Benam and Horgan, 2022b), motivating the extension of its application to *compressible* elastomers in the current work. It is readily noted that in the limit as $N \to \infty$, then $\mu = \mu_0$ and the model in Eq. (5) simplifies to the classical neo-Hookean strain energy function. Within the framework of Eq. (4), the *deviatoric* form of this model becomes:

$$W_{Dev}(\bar{I}_1) = \frac{3(n-1)}{2n}\mu N\left[\frac{1}{3N(n-1)}(\bar{I}_1 - 3) - \ln\left(\frac{\bar{I}_1 - 3N}{3-3N}\right)\right]. \tag{8}$$

The model in Eq. (8), is of the generalised neo-Hookean type $W(I_1)$. It is well recognised that a robust strain energy function W has to include an I_2 term in its functional form too; i.e., $W \equiv W(I_1, I_2)$. See, e.g., Anssari-Benam et al. (2021c) and references cited therein for a review on the role of I_2 in constitutive modelling. Furthermore, as outlined by Destrade et al. (2017), the inclusion of an I_2 term is also expedient from the perspective of compatibility with fourth-order weakly nonlinear elasticity. Accordingly, we consider the following I_2 term $g(I_2)$ as an adjunct to $W(I_1)$ of Eq. (5):

$$g(I_2) = C_2 \ln\left(\frac{I_2}{3}\right). \tag{9}$$

This term has been proposed by Gent and Thomas (1958) and Pucci and Saccomandi (2002) in the context of modelling the mechanical behaviour of *incompressible* rubber-like materials, and its versatility in improving the modelling results when used in conjunction with a special form of the model in Eq. (5) has been demonstrated in our preceding publications (see Anssari-Benam et al., 2021a; 2021b). Within the framework of Eq. (4), therefore, the *deviatoric* form of $W_{Dev}(\bar{I}_1, \bar{I}_2)$ using the *parent* model in Eq. (5) and the $g(I_2)$ term in Eq. (9) becomes:

$$W_{Dev}(\bar{I}_1, \bar{I}_2) = \frac{3(n-1)}{2n}\mu N\left[\frac{1}{3N(n-1)}(\bar{I}_1 - 3) - \ln\left(\frac{\bar{I}_1 - 3N}{3-3N}\right)\right] + C_2 \ln\left(\frac{\bar{I}_2}{3}\right). \tag{10}$$

For the *volumetric* part W_{Vol}, we consider the following functional form:

$$W_{Vol}(J) = \frac{K}{4}(J^2 - 1 - 2\ln J), \tag{11}$$

where K is associated with the bulk modulus. Note that the functional form of $W_{Vol}(J)$ in Eq. (11) corresponds to setting $\beta = -2$ in the fourth entry of Table 1. The choice for W_{Vol} is obviously not unique. However, our impetus in considering this specific function is two-fold. First, it is natural to require that $W_{Vol}(J)$ should approach infinity as $J \to \infty$ or $J \to 0$. The W_{Vol} function in Eq. (11) satisfies this requirement. Second, this functional form appears to be a well-established W_{Vol} term used in FE analyses; see, e.g., the FEAP manual (Taylor, 2013).

Thus, the final form of the family of models considered for application to the mechanical behaviour of *compressible* elastomers becomes:

$$\begin{cases} W = \dfrac{3(n-1)}{2n}\mu N\left[\dfrac{1}{3N(n-1)}(\bar{I}_1 - 3) - \ln\left(\dfrac{\bar{I}_1 - 3N}{3-3N}\right)\right] + \dfrac{K}{4}(J^2 - 1 - 2\ln J)\,, \\ W = \dfrac{3(n-1)}{2n}\mu N\left[\dfrac{1}{3N(n-1)}(\bar{I}_1 - 3) - \ln\left(\dfrac{\bar{I}_1 - 3N}{3-3N}\right)\right] + C_2\ln\left(\dfrac{\bar{I}_2}{3}\right) + \dfrac{K}{4}(J^2 - 1 - 2\ln J)\,. \end{cases} \tag{12}$$

For simplicity, we will henceforth refer to the models in Eqs. $(12)_1$ and $(12)_2$ as *Model I* and *Model II*, respectively. Note that *Model I* contains four model parameters, while *Model II* has five parameters. Many other forms of this family of W may readily be constructed on using specific prescribed values of n (see the remark below) in the *parent* model Eq. (5), and other choices of I_2 term $g(I_2)$ in Eq. (9).

Remark. As demonstrated by Anssari-Benam and Horgan (2022b), in the limit $n \to \infty$ the model in Eq. (5) reduces to the celebrated Gent (1996) model:

$$\lim_{n\to\infty} W_{Inc} = -\frac{1}{2}J_m\mu_0 \ln\left[1 - \frac{I_1 - 3}{J_m}\right]. \tag{13}$$

Similarly, on setting $n = 3$ in Eq. (5), we recover the model utilised by Anssari-Benam and Bucchi (2021) as:

$$\underset{n=3}{W_{Inc}} = \mu N\left[\frac{1}{6N}(I_1 - 3) - \ln\left(\frac{I_1 - 3N}{3-3N}\right)\right], \tag{14}$$

which is a special case of the nonaffine network model of Davidson and Goulbourne (2013). This model has been successfully applied to modelling the deformation of soft tissues (see, e.g., Anssari-Benam and Bucchi, 2018) as well as rubber-like materials (Anssari-Benam and Bucchi, 2021; Anssari-Benam et al., 2021b). Horgan (2021) has also demonstrated that the first

derivative of this model differs from that of the Gent model by only a constant. However, the model in Eq. (5) is a higher order, and therefore a more accurate, Padé approximation of the non-Gaussian chain mechanics. See also Anssari-Benam and Horgan (2022a) for a hierarchy of the order of the Padé approximants in the response functions of some of the existing generalised neo-Hookean limiting chain extensibility models. It is therefore observed that the model in Eq. (5), or equivalently Eq. (8) in the *deviatoric* form, is the *parent* to many of the limiting chain extensibility models in the literature, in both of their *incompressible* and *deviatoric* forms. If the models in Eqs. (13) and (14) were used in Eq. (12), then the minimum number of model parameters for this family of models would reduce even further to three, in the case of $W(\overline{I_1}, J)$, and four in the case of $W(\overline{I_1}, \overline{I_2}, J)$.

The compatibility of the proposed family of strain energy functions W in Eq. (12) with *slight* compressibility effects may be demonstrated on adopting the approach by Horgan and Murphy (2007a). Under tensile deformation, an empirical kinematic relationship has been found to hold true for *slightly* compressible elastomers in the form $\lambda_S = \lambda_T^{-\frac{1}{2}+\epsilon}$ (Beatty and Stalnaker, 1986), where λ_T denotes the axial stretch and λ_S is the lateral stretch in the two remaining perpendicular directions. The value of ϵ is found to be small; i.e., $\epsilon \ll 1$ (Beatty and Stalnaker, 1986). Based on these findings, Horgan and Murphy (2007a) stipulate that "*it is reasonable to expect that any kinematic relation for almost incompressible behaviour should reduce [at the very least] to the first-order equivalent*" of the foregoing relationship; i.e., $\lambda_S^{(1)} = \lambda_T^{-\frac{1}{2}} \ln \lambda_T$. They also show that for a strain energy function written in the form: $W = \mu\psi(\lambda_1, \lambda_2, \lambda_3) + Kf(J)$, the first-order term $\lambda_S^{(1)}$ is obtained as (Horgan and Murphy, 2007a):

$$\lambda_S^{(1)} = -\frac{1}{2\lambda_T}\psi_2\left(\lambda_T, \lambda_T^{-\frac{1}{2}}, \lambda_T^{-\frac{1}{2}}\right), \tag{15}$$

where the subscript '2' denotes partial differentiation with respect to the second principal stretch. For *Model I*, the function $\psi(\lambda_1, \lambda_2, \lambda_3)$ takes the form:

$$\psi(\lambda_1, \lambda_2, \lambda_3) = \frac{3N(n-1)}{2n}\left[\frac{1}{3N(n-1)}\left(J^{-\frac{2}{3}}I_1 - 3\right) - \ln\left(\frac{J^{-\frac{2}{3}}I_1 - 3N}{3-3N}\right)\right], \tag{16}$$

with:

$$J = \lambda_1\lambda_2\lambda_3 \quad , \quad I_1 = \lambda_1^2 + \lambda_2^2 + \lambda_3^2 \,. \tag{17}$$

It follows that:

$$\lambda_S^{(1)} = -\frac{3Nn\lambda_T(\lambda_T^3 - 1) - \lambda_T^3(\lambda_T^3 + 1) + 2}{6n\lambda_T^{\frac{3}{2}}(\lambda_T^3 - 3N\lambda_T + 2)}. \tag{18}$$

Similarly, for *Model II* the function $\psi(\lambda_1, \lambda_2, \lambda_3)$ is:

$$\psi(\lambda_1, \lambda_2, \lambda_3) = \frac{3N(n-1)}{2n}\left[\frac{1}{3N(n-1)}\left(J^{-\frac{2}{3}}I_1 - 3\right) - \ln\left(\frac{J^{-\frac{2}{3}}I_1 - 3N}{3 - 3N}\right)\right] + C\ln\left(\frac{J^{-\frac{4}{3}}I_2}{3}\right), \tag{19}$$

where C is a dimensionless parameter defined as: $C = C_2/\mu$, J and I_1 are as in Eq. (17) and $I_2 = \lambda_1^2\lambda_2^2 + \lambda_2^2\lambda_3^2 + \lambda_1^2\lambda_3^2$. We therefore find that:

$$\lambda_S^{(1)} = -\frac{(\lambda_T - 1)(\lambda_T^2 + \lambda_T + 1)[3N\lambda_T n(2\lambda_T^3 + 2C\lambda_T + 1) - 2C\lambda_T n(\lambda_T^3 + 2) - \lambda_T^3(2\lambda_T^3 + 5) - 2]}{6n\lambda_T^{\frac{3}{2}}(\lambda_T^3 - 3N\lambda_T + 2)(2\lambda_T^3 + 1)}. \tag{20}$$

The plots in Fig. 1 compare the experimentally observed trend versus the *typical* predicted kinematical relationship between the axial and lateral stretches, λ_T and λ_S, using Eqs. (18) and (20) for the case of *slight* compressibility. It is observed that, except for *Model I* in the compression range ($\lambda_T < 1$), the proposed family of models favourably capture the empirical kinematics between the axial and lateral stretches for *slightly* compressible elastomers under tensile deformation. Note that, as outlined by Horgan and Murphy (2007a; 2007b; 2009a; 2009b; 2009c; 2009d), the predictions of many of the existing models in the literature do *not* agree with this experimental kinematical trend.

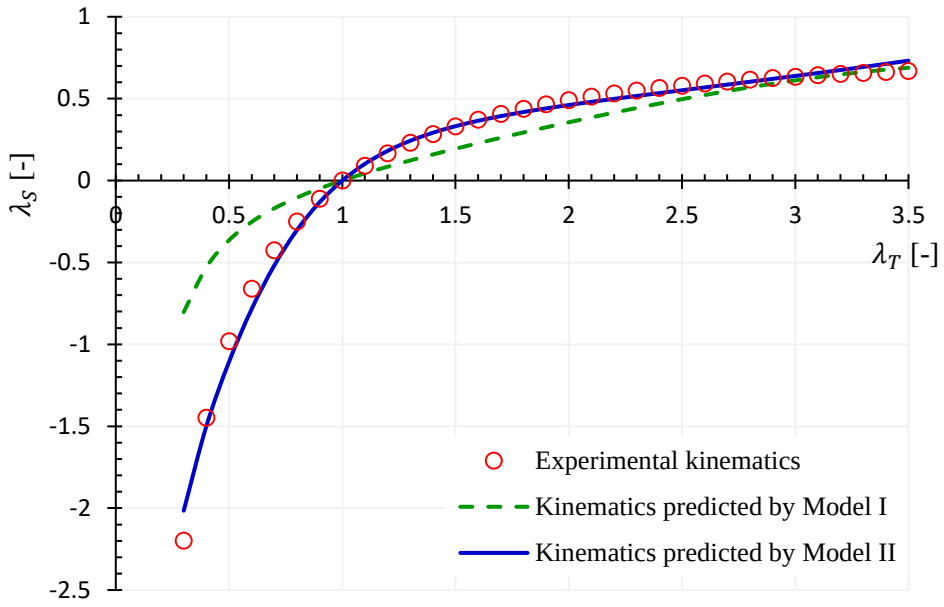

Fig. 1. Comparison between the first-order kinematical relationship observed in experiments and the predictions of *Models I* and *II* for slightly compressible elastomers under simple tension. The axial stretch is λ_T, while λ_S denotes the lateral stretch. The plots indicate the correlation between Eqs. (18) and (20), for *Models I* and *II*, respectively, and the experimental trend ($\lambda_S = \lambda_T^{-\frac{1}{2}} \ln \lambda_T$). *Model II* provides the most favourable correlation, while *Model I* appears suitable for the tensile range ($\lambda_T > 1$). Note that these results are *typical* predictions, obtained at $\mu_0/\mu = 0.92$ and 2.32 for *Models I* and *II*, respectively. All valid combinations of the model parameters n, N and C_2 resulting in these ratios produce a similar trend.

With the functional form of the family of models now at hand, given by Eq. (12), the ensuing Cauchy stress tensor **T** may be obtained from W using (see, e.g., Penn, 1970; Peng and Landel, 1975):

$$\mathbf{T} = \frac{2}{J}\left[\left(\frac{1}{3}\bar{I}_2 W_{\bar{2}} - \frac{1}{3}\bar{I}_1 W_{\bar{1}} + \frac{1}{2} J W_J\right)\mathbf{I} + J^{-\frac{2}{3}} W_{\bar{1}}\,\mathbf{B} - J^{\frac{2}{3}} W_{\bar{2}}\,\mathbf{B}^{-1}\right], \tag{21}$$

where $W_{\bar{1}}$ and $W_{\bar{2}}$ indicate the partial derivatives of W with respect to the *deviatoric* invariants $\bar{I}_1$ and $\bar{I}_2$, and W_J signifies $\partial W/\partial J$. Note that **B** is the usual left Cauchy-Green deformation tensor, and *not* the deviatoric counterpart. This representation is more convenient for correlation with the experimental data, as the data is almost always measured and reported with respect to λ_i and *not* the deviatoric measure $\bar{\lambda}_i$.

3. Correlation with experimental data

In modelling the finite deformation of *compressible* elastomers, more detailed experimental data is required compared with the incompressible case. In particular, information regarding the lateral stretches λ_T plays a key role in computing J, and therefore in correctly characterising the contributions of both *deviatoric* and *volumetric* parts of W. While many studies may be found in the literature which report on the simple tension/compression of polymeric foams and gels, far fewer include the information on the lateral stretches λ_T. This problem is often further exacerbated when data regarding additional concurrent deformation modes are sought. Here, however, we demonstrate the application of the proposed family of models to extant experimental datasets on uniaxial tension (El-Ratal and Mallick, 1996), uniaxial and equi-biaxial compression (Kossa and Berezvai, 2016), and uniaxial and simple shear deformations (Yan et al. 2021) of polymeric foams, which include the lateral stretches λ_T. Similarly, we consider uniaxial tension (Urayama et al., 1993), and uniaxial and simple shear deformations (Upadhyay et al., 2020) for polymeric gels.

Accordingly, for the aforementioned deformations we note that:

$$\begin{cases} J = \lambda\lambda_T^2\,, \;\; I_1 = \lambda^2 + 2\lambda_T^2\,, \;\; I_2 = \lambda^{-2} + 2\lambda_T^{-2}\,, \;\; \text{for uniaxial deformation,} \\ J = \lambda^2\lambda_T\,, \;\; I_1 = 2\lambda^2 + \lambda_T^2\,, \;\; I_2 = 2\lambda^{-2} + \lambda_T^{-2}\,, \;\; \text{for equi} - \text{biaxial deformation,} \\ J = 1\,, \;\; I_1 = I_2 = 3 + \gamma^2\,, \;\; \text{for simple shear,} \end{cases} \tag{22}$$

where λ, λ_T and γ are the axial stretch, lateral stretch and the amount of shear, respectively. On using Eq. (21), the (Cauchy) stress – deformation relationships for *Model I* follow:

$$(T)_m = \frac{2}{(J)_m}\left[\frac{1}{2n}\mu\,\frac{(\bar{I_1})_m - 3Nn}{(\bar{I_1})_m - 3N}\left(J^{-\frac{2}{3}}\lambda^2 - \frac{1}{3}\bar{I_1}\right)_m + \frac{K}{4}(J^2-1)_m\right], \tag{23}$$

where the subscript m indicates the mode of deformation, i.e., uniaxial, equi-biaxial and/or simple shear, and $(J)_m$ and $(\bar{I_1})_m$ are obtained via Eq. (22). Note that for simple shear, where $J = 1$, Eq. (23) coincides with the better-known counterpart relationship for the incompressible case, namely:

$$T_{ss} = 2\gamma\frac{\partial W}{\partial I_1} = 2\gamma\left(\frac{1}{2n}\mu\,\frac{I_1 - 3Nn}{I_1 - 3N}\right), \tag{24}$$

where the subscript *ss* denotes simple shear. See also Horgan and Murphy (2010) on this point.

The counterpart relationships for *Model II* are:

$$(T)_m = \frac{2}{(J)_m}\left[\frac{1}{2n}\mu\,\frac{(\bar{I}_1)_m - 3Nn}{(\bar{I}_1)_m - 3N}\left(J^{-\frac{2}{3}}\lambda^2 - \frac{1}{3}\bar{I}_1\right)_m + C_2\left(\frac{1}{3} - \frac{J^{\frac{2}{3}}\lambda^{-2}}{\bar{I}_2}\right) + \frac{K}{4}(J^2-1)_m\right], \tag{25}$$

where again the subscript m indicates the mode of deformation, i.e., uniaxial, equi-biaxial and/or simple shear, and $(J)_m$ and $(\bar{I}_1)_m$ and $(\bar{I}_2)_m$ are obtained via Eq. (22). Equivalently, for simple shear we have:

$$T_{ss} = 2\gamma\left(\frac{\partial W}{\partial I_1} + \frac{\partial W}{\partial I_2}\right) = 2\gamma\left(\frac{1}{2n}\mu\,\frac{I_1 - 3Nn}{I_1 - 3N} + \frac{C_2}{I_2}\right). \tag{26}$$

In the proceeding sections, Eqs. (23) to (26) will be used for simultaneous fitting to the pertinent experimental datasets. The best fit is achieved by minimising the residual sum of squares (RSS) function defined as: $\text{RSS} = \sum_i \left(T^{model} - T^{experiment}\right)_i^2$, where *i* is the number of data points. The minimisation is performed via an in-house developed code in MATLAB®, using the genetic algorithm (GA) toolbox. The Coefficient of determination R^2 is used as the measure for the goodness of the fits. The presented relative error (%) in the plots is calculated as: $\left|\frac{T^{model} - T^{experiment}}{T^{experiment}}\right| \times 100$.

3.1. Polymeric Foams

We start by the dataset due to El-Ratal and Mallick (1996) for polyurethane foams in uniaxial tension. Therein they report on two types of the foam, namely an industrial and a commercial sample. We undertook fitting the models to these datasets using Eqs. $(22)_1$, (23) and (25). The tabulated data, reproduced from El-Ratal and Mallick (1996), has been presented in Table A1, Appendix A, for both samples. The plots in Fig.2 show the modelling results, and Table 2 summarises the model parameters. Both models provide a favourable fit, with no particular advantage of *Model II* over *Model I*. Indeed, we note that the values of the parameter C_2 are close to zero, and hence both models provide a similar correlation with the data.

Table 2 – Model parameter values for industrial and commercial polyurethane foam samples under uniaxial tension due to El-Ratal and Mallick (1996).

	Industrial polyurethane foam sample					
	μ [kPa]	N [-]	n [-]	C_2 [kPa]	K [kPa]	R^2
Model I	58.89	7.94	0.38	-	4.04	0.99
Model II	60.21	12.53	0.25	7.19×10^{-5}	4.16	0.99
	Commercial polyurethane foam sample					
	μ [kPa]	N [-]	n [-]	C_2 [kPa]	K [kPa]	R^2
Model I	34.54	1.10	0.98	-	1×10^{-4}	0.99
Model II	34.56	1.10	0.98	2.56×10^{-5}	9×10^{-5}	0.99

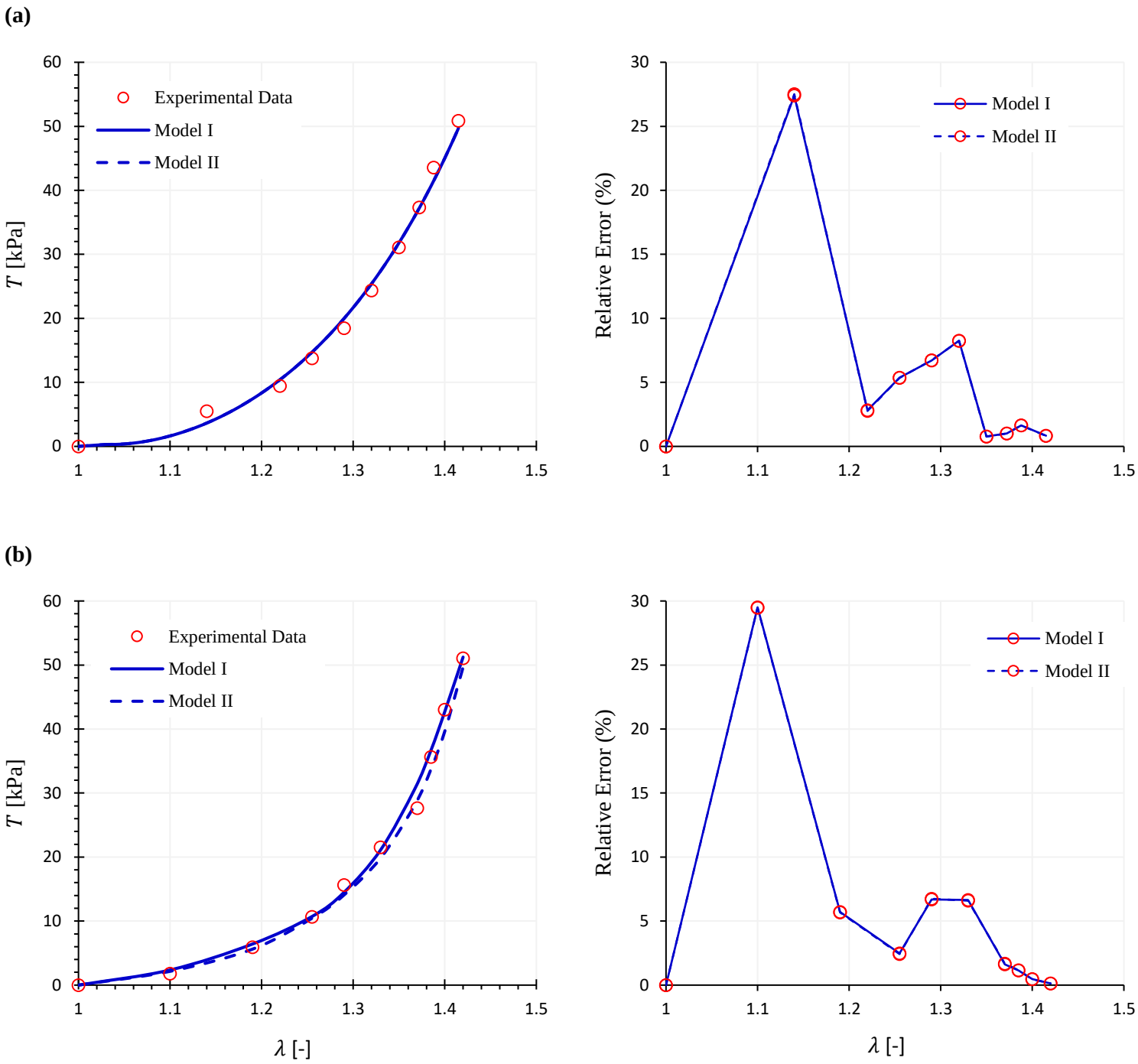

Fig. 2. Modelling results for: (a) industrial; and (b) commercial polyurethane foam samples due to El-Ratal and Mallick (1996) under uniaxial tension. Note that the value of C_2 is close to zero for both datasets, rendering the provided fits by both models to coincide (as well as the relative errors).

Next we present the modelling results for uniaxial and equi-biaxial compression of a polyethylene foam sample due to Kossa and Berezvai (2016). The numerical data, reproduced from Kossa and Berezvai (2016), are presented in Table A2 of Appendix A. Using Eqs. (22), (23) and (25), each model was simultaneously fitted to the two deformation modes. Plots in

Fig. 3 demonstrate the obtained fits, with model parameters given in Table 3. Again, it is observed that both models provide a favourable fit to the data, with no tangible advantage of one model over the other; note from Table 3 that the value of C_2 is comparably small. The foregoing two datasets indicate that the addition of an I_2 term *does not always* result in an improved fit to the data.

Table 3 – Model parameter values for a polyethylene foam sample due to Kossa and Berezvai (2016) under uniaxial and equi-biaxial compression.

	Polyethylene foam sample					
	μ [MPa]	N [-]	n [-]	C_2 [MPa]	K [MPa]	R^2 (Uni – Bi)
Model I	23.59	0.29	1.13	-	169.29	0.98 – 0.99
Model II	23.41	0.29	1.13	3.77×10^{-5}	169.30	0.98 – 0.99

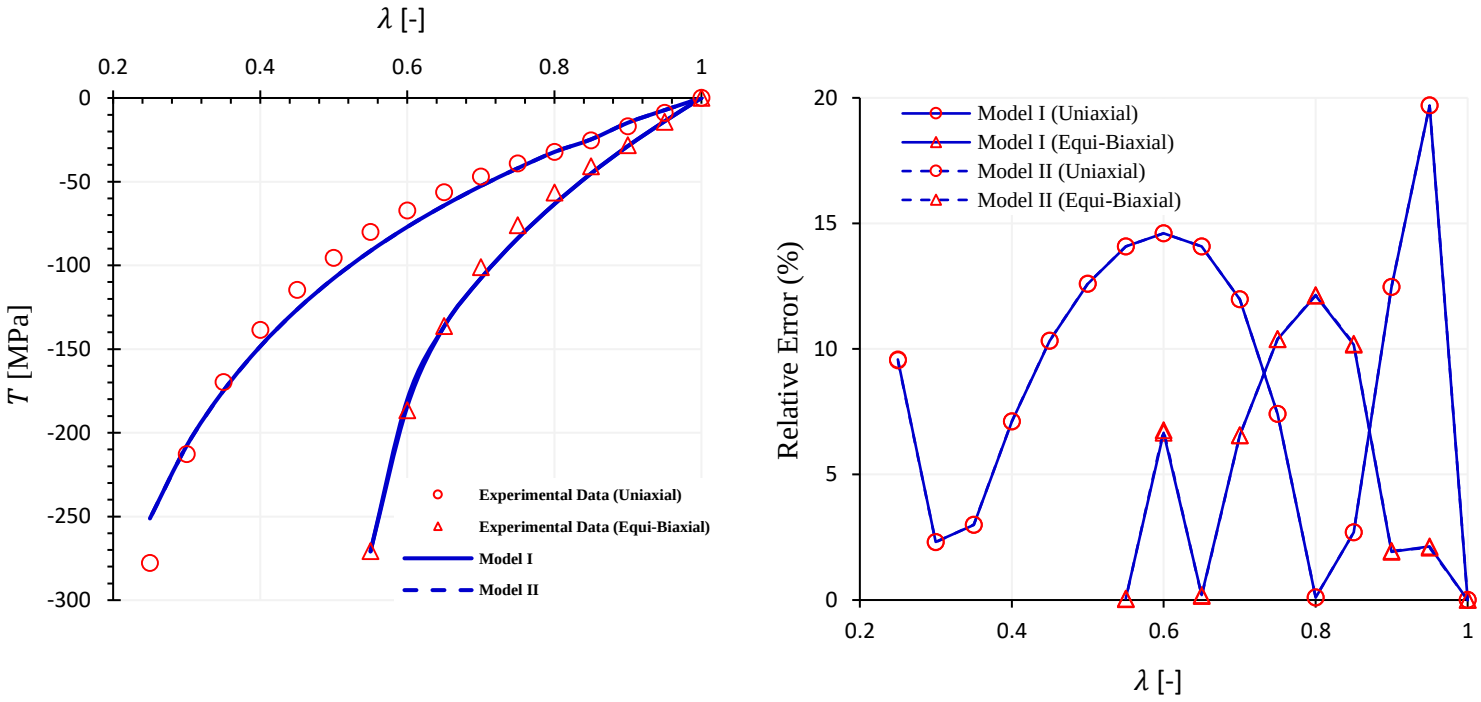

Fig. 3. Modelling results for a polyethylene foam sample under uniaxial and equi-biaxial compression due to Kossa and Berezvai (2016). Note that the value of C_2 for this dataset is close to zero which renders the fits to coincide for both models (and the relative errors too).

The third dataset for polymeric foams we consider here is due to Yan et al. (2021), reporting on uniaxial and simple shear deformations. The tabulated dataset extracted from that study is

presented in Table A3, Appendix A. *Models I* and *II* were each simultaneously fitted to the two datasets using Eqs. (22) to (26). The modelling results are presented in Fig. 4, and Table 4 contains the model parameters. While both models provide a favourable fit, *Model II* provides a noticeable improvement compared with *Model I*. For this dataset, therefore, it appears that the inclusion of the I_2 has proved to be advantageous. The intricate behaviour of this specimen may be more appreciated by noting that Yan et al. (2021) obtained their best fit on using a three-term Ogden hyperfoam model, which corresponds to *nine* model parameters. *Models I* and *II*, with four and five parameters, respectively, appear to provide comparably favourable fits.

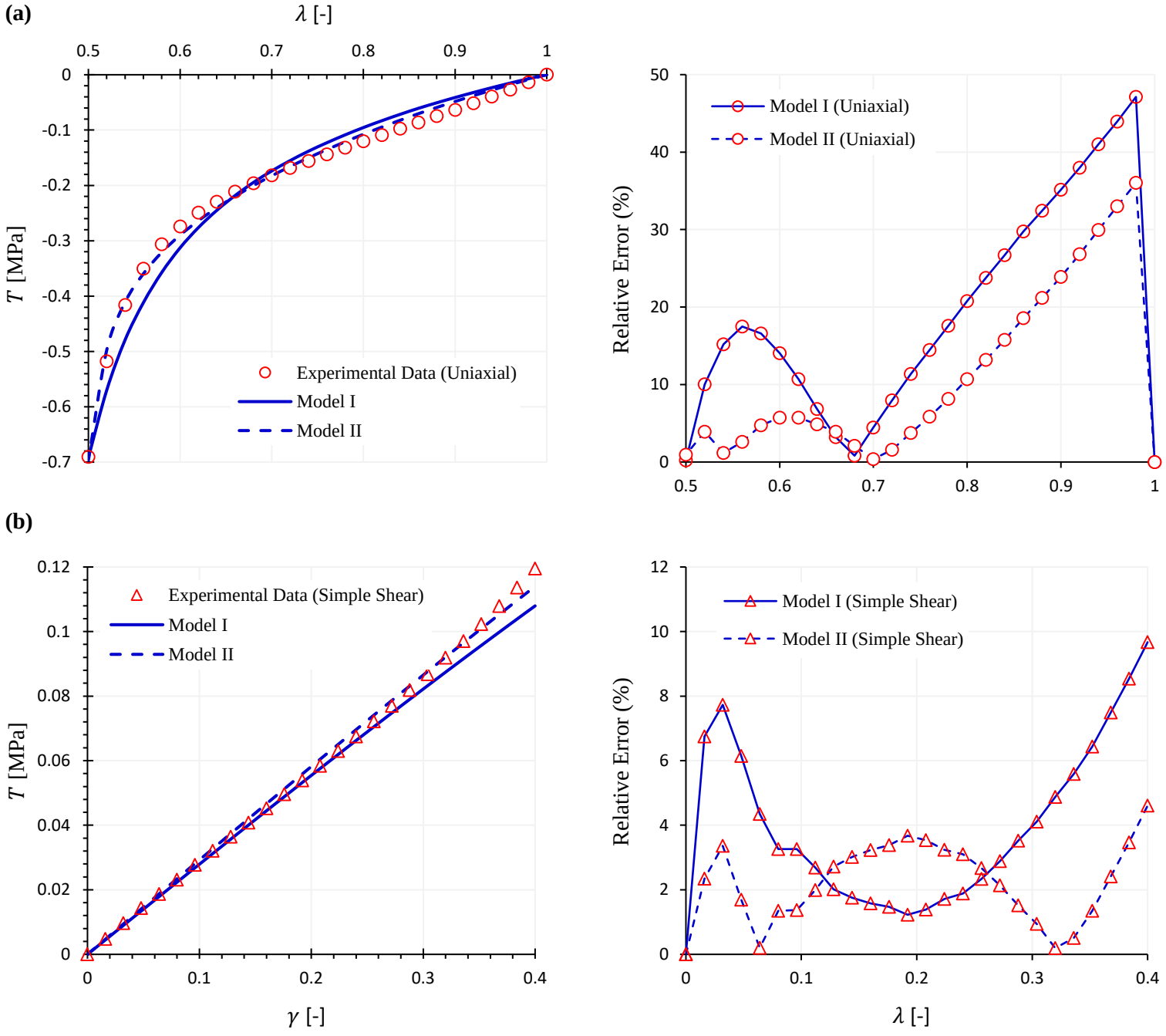

Fig. 4. Modelling results for a polymeric foam sample under: (a) uniaxial and; (b) simple shear deformations, due to Yan et al. (2021).

Table 4 – Model parameter values for a polymeric foam sample due to Yan et al. (2021) under uniaxial and simple shear deformations. Note that R^2 values are ordered for the uniaxial and simple shear deformation datasets (Uni – SS).

	μ [MPa]	N [-]	n [-]	C_2 [MPa]	K [MPa]	R^2 (Uni – SS)
Model I	0.11	0.55	0.59	-	0.35	0.97 – 0.99
Model II	0.15	0.58	0.91	0.17	0.35	0.99 – 0.99

We also note here the work of Zhang et al. (1997; 1998), where the uniaxial compression, tension and simple shear deformations of a polystyrene foam specimen have been experimentally characterised. Unfortunately, the information regarding the lateral stretch λ_T or J has not been included therein. However, the reported simple shear deformation of the specimen exhibits an interesting behaviour; see figure 13 of Zhang et al. (1998). In essence, the data shows an instability similar to the *limit-point* instability in inflation of thin rubber-like balloons (see, e.g., Anssari-Benam et al., 2021b), where the shear stress reaches a maximum and upon further shearing the stress decreases. The existence of such instability was predicted by the modelling approach in a prior study by the authors (Anssari-Benam and Horgan, 2021). However, no attempt was made therein to model a dataset. While the data in Zhang et al. (1998) indicates rate-sensitivity in the shear deformation of the polystyrene foam specimen, we collated the data points from their quasi-static shear deformation tests as the elastic behaviour baseline. The tabulated data is given in Table A4 of Appendix A. Since the simple shear deformation is isochoric, this deformation can be modelled without λ_T or J data. On using Eqs. $(22)_3$, (24) and (26), *Models I* and *II* were fitted to this dataset. The results are shown in Fig. 5, and model parameters are summarised in Table 5. It is observed that both models importantly capture this instability, and provide excellent fits to the data. Capturing this behaviour using a hyperelastic model, to the knowledge of the authors, has not been demonstrated in the literature and is unique to the proposed models herein.

Table 5 – Model parameter values for a polystyrene foam specimen due to Zhang et al. (1998) under simple shear deformation.

	μ [MPa]	N [-]	n [-]	C_2 [MPa]	R^2
Model I	0.07	0.99	0.92	-	0.99
Model II	0.07	0.99	0.92	0.02_5	0.99

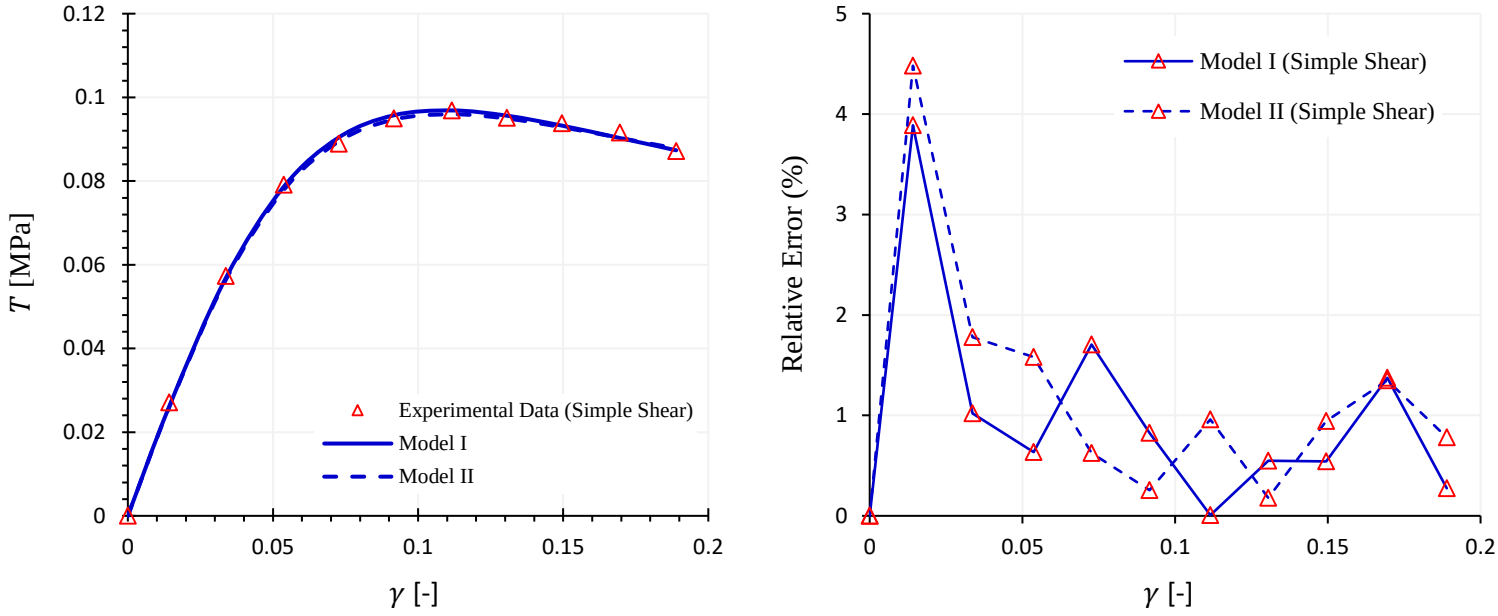

Fig. 5. Modelling the instability in simple shearing of a compressible polystyrene foam specimen due to Zhang et al. (1998).

3.2. Polymeric gels

Similar problems as with the datasets pertaining to the deformation of foams are also encountered in relation to gels, in that information regarding the lateral stretches λ_T (or J) are often not reported in the literature. However, here we consider two datasets from hydrogel-based specimens under uniaxial tension and simple shear, due to Urayama et al. (1993) and Upadhyay et al. (2020).

Starting with the former, Urayama et al. (1993) report on uniaxial tension of Poly(Vinyl Alcohol) gel specimens; PVA hydrogels. The tabulated data extracted from that study has been presented in Table A5, Appendix A. Note that therein they report the value of the Poisson ratio for this specimen as $\nu = 0.338$, from which the lateral stretch λ_T was calculated using the relationship $\lambda_T = \lambda^{-\nu}$ (Urayama et al., 1993). The plots in Fig. 6 show the modelling results using both *Models I* and *II*, and Table 6 summarises the model parameters. While both models provide a favourable fit, *Model II* proves more advantageous for this dataset.

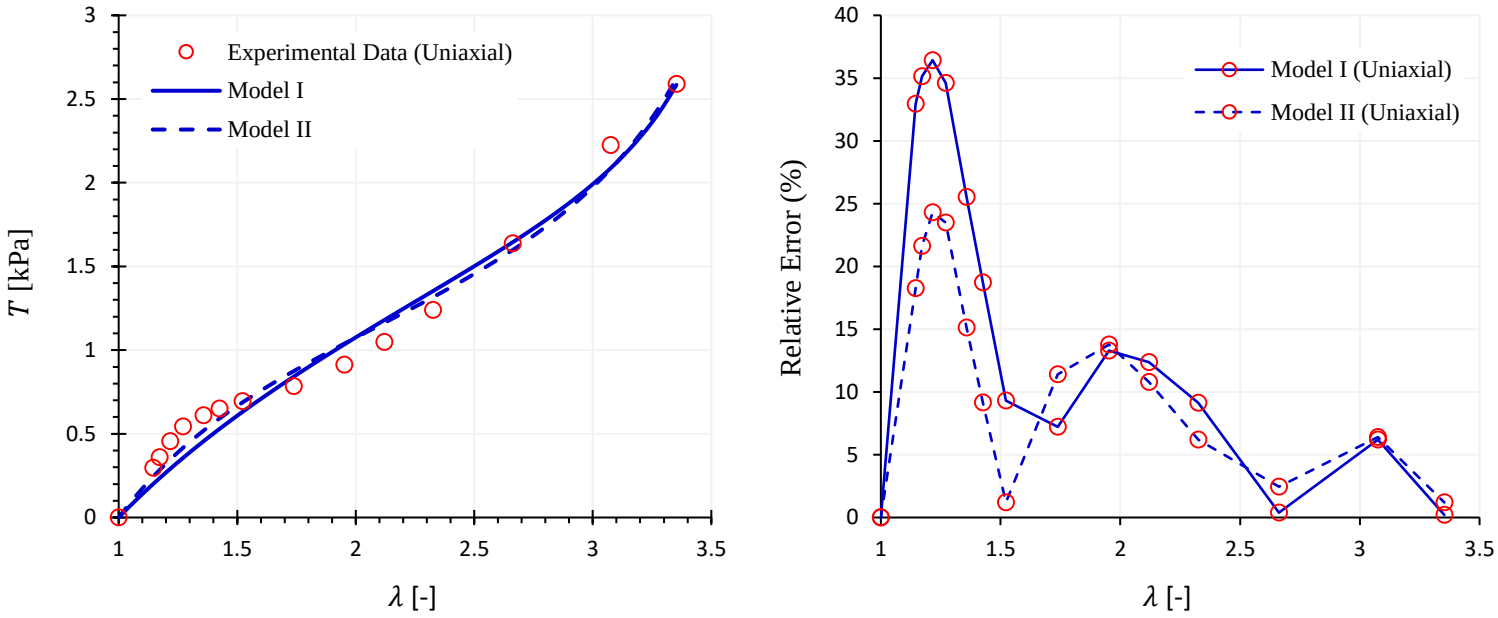

Fig. 6. Modelling results for a PVA gel specimen under uniaxial tension due to Urayama et al. (1993).

Table 6 – Model parameter values for the PVA gel specimen due to Urayama et al. (1993) under uniaxial deformation.

	μ [kPa]	N [-]	n [-]	C_2 [kPa]	K [kPa]	R^2
Model I	0.11	6.95	17.65	-	4.00	0.97
Model II	0.28	8.22	38.18	1.07	1.01	0.98

Next we consider the uniaxial tension/compression and simple shear datasets due to Upadhyay et al. (2020). Unfortunately, information regarding the lateral stretches has not been provided therein. However, for hydrogel-based constructs, one may find a Poisson ratio ν

within the range $0.3 < \nu < 0.5$ for hydrogel-based constructs in the literature (see, e.g., Urayama et al., 1993; Normand et al., 2000; Cai et al., 2010). Within this range, we choose a value of $\nu = 0.45$, from which we compute the lateral stretches via $\lambda_T = \lambda^{-\nu}$. The extracted tabulated data has been included in Appendix A, Table A6. The modelling results using both *Models I* and *II* are presented in Fig. 7, and the model parameters have been given in Table 7. It is observed that both *Models I* and *II* provide a virtually identical fit to the dataset (the dotted and solid curves coincide) and so there is no particular advantage for *Model II* over *Model I*. It must be noted that changing the value of ν does not impede the capability of the models in capturing these datasets; however, we refrain from repeating the modelling results here.

(a)

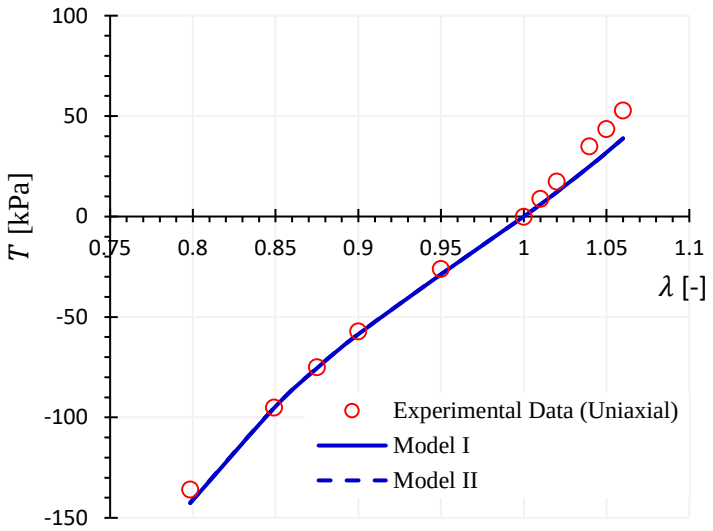

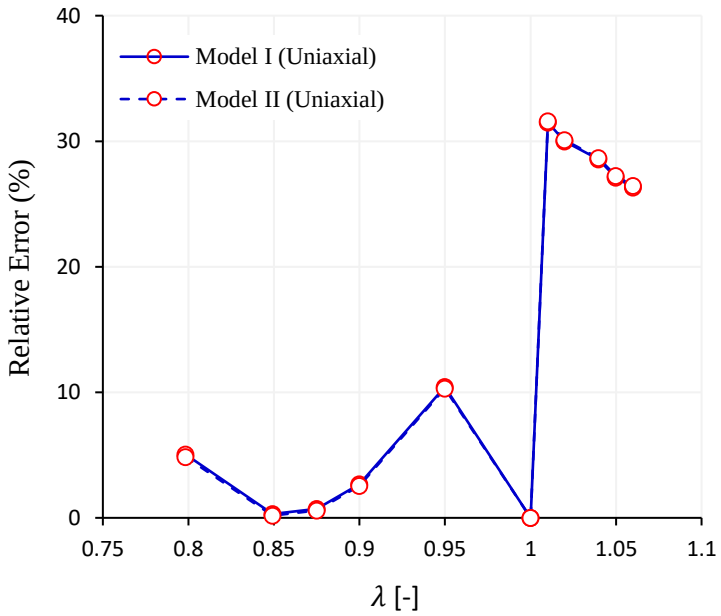

(b)

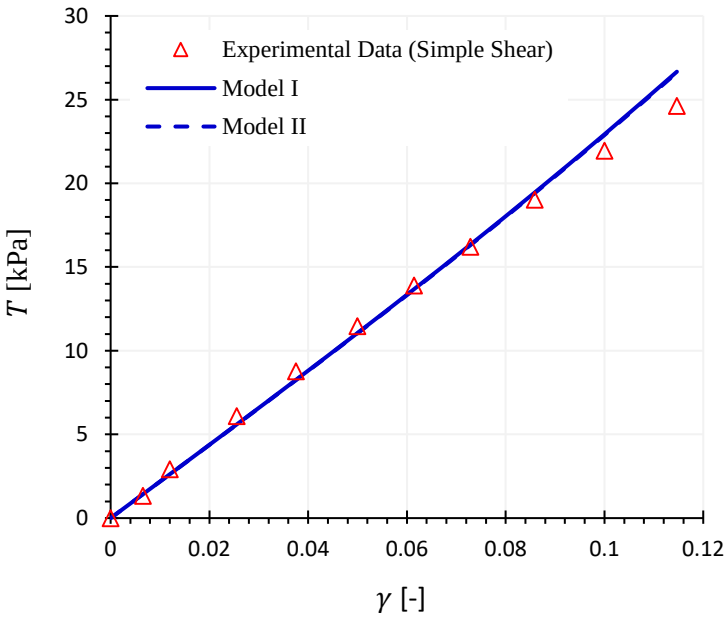

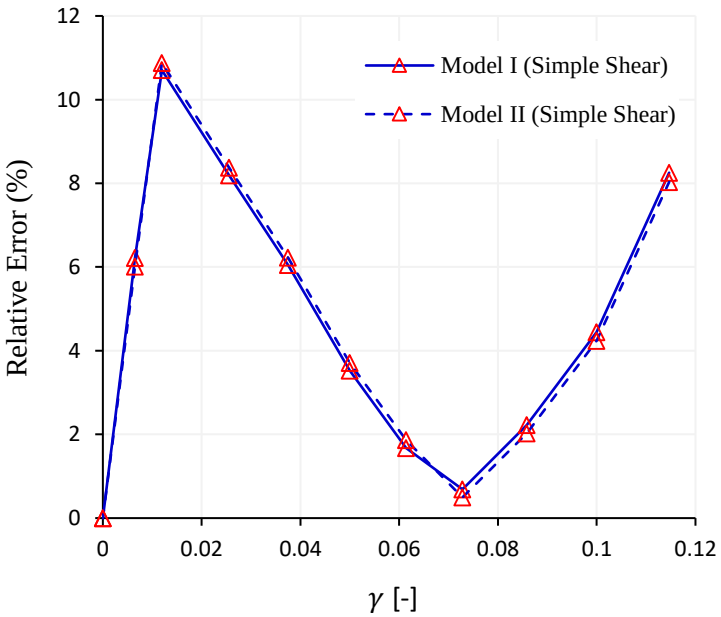

Fig. 7. Modelling results for a hydrogel sample under: (a) uniaxial and; (b) simple shear deformations, due to Upadhyay et al. (2020).

Table 7 – Model parameter values for the hydrogel sample due to Upadhyay et al. (2020) under uniaxial and shear deformations.

	μ [kPa]	N [-]	n [-]	C_2 [kPa]	K [kPa]	R^2 (Uni – SS)
Model I	647.08	0.89	1.08	-	2026.30	0.98 – 0.99
Model II	625.32	0.89	1.08	9.43×10^{-4}	2026.10	0.98 – 0.99

In passing we also note the uniaxial tension dataset due to Sun et al. (2012), which reports on the deformation of alginate-polyacrylamide hydrogels undergoing elastic deformations up to very high stretch levels of $\lambda \approx 23$. To conclude our modelling analysis, we include this dataset here. Again, we note that since the lateral stretches have not been reported in that study, we take $\nu = 0.45$ and compute the lateral stretches using $\lambda_T = \lambda^{-\nu}$ accordingly. See Table A7 of Appendix A for the tabulated data. The modelling results are shown in Fig. 8, and the model parameters presented in Table 8. Again we note that modelling predictions for both *Models I* (solid line) and *II* (dotted line) coincide, with no particular advantage in using Model *II* over *Model I*.

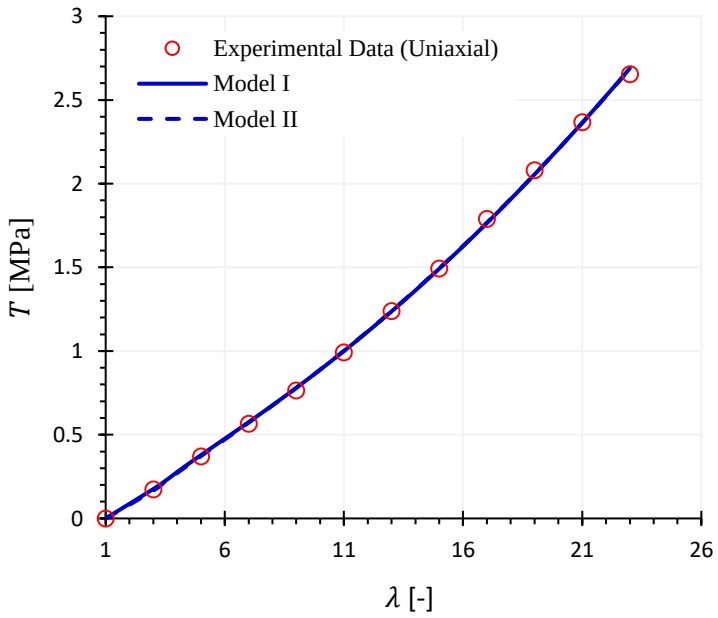

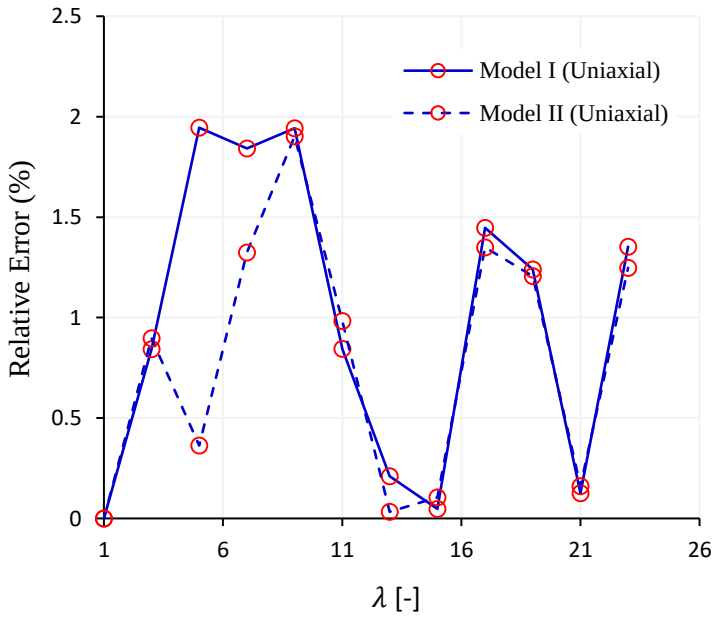

Fig. 8. Modelling results for an alginate-polyacrylamide hydrogel specimen under uniaxial tension up to very large stretch levels ($\lambda \approx 23$) due to Sun et al. (2012).

Table 8 – Model parameter values for the alginate-polyacrylamide hydrogel specimen due to Sun et al. (2012) under uniaxial deformation.

	μ [MPa]	N [-]	n [-]	C_2 [MPa]	K [MPa]	R^2
Model I	0.07	1.02	4.93	-	1.84	0.99
Model II	0.27	0.32	19.99	0.01	1.96	0.99

4. Concluding remarks

The application of a new family of models, given in Eq. (12), to the finite deformation of compressible elastomers was explored in this study. The proposed family of models is based on an incompressible three-parameter *parent* strain energy function W (Anssari-Benam, 2021; Anssari-Benam and Horgan, 2022b), extended here to the compressible case via an additive split of W into a *deviatoric* and a *volumetric* contribution. Subject to the requirements detailed in Section 2, the models were developed and applied to extant deformation datasets of polymeric foams and gels. The favourable correlation between the model predictions and the experimental data was demonstrated in Section 3.

Of the advantages pertaining to the proposed family of models, the number of model parameters is perhaps an obvious one. The considered functional forms in Eq. (12) contain four and five model parameters for *Models I* and *II*, respectively. The proposed models were also shown to be the *parent* to other limiting chain extensibility models in the literature such as the Gent (1996) model and that of Anssari-Benam and Bucchi (2021); see the Remark in Section 2. If these sub-set functional forms are used instead of the parent form in (12), then the number of model parameters will further reduce to three and four, respectively. With such relatively low number of parameters, the considered family of models herein demonstrated a promising capability in capturing the deformation behaviour of compressible elastomers. For the polymeric foam considered by Yan et al. (2021), as an example, the Ogden hyperfoam model of the third order, leading to nine model parameters, was required to provide a favourable fit

to the uniaxial and simple shear deformation datasets. *Model II*, with only five model parameters, proved equally capable of providing such a favourable fit; see Fig. 4. Other studies, too, have identified models with a high number of parameters suitable for application to, for example, polyurethane foams with more than six parameters (see., e.g., Ding et al., 2021). With lower number of model parameters, the proposed family of models herein will help alleviating the optimisation issues and fitting sensitivities.

Another advantage of the proposed family of models is the robustness that they provide for modelling various deformation behaviours of a wide range of elastomers. Polymeric foams have a distinct mechanical behaviour from their hydrogel counterparts. Yet, the considered models here were capable of predicting the experimental datasets of this wide variety. Moreover, challenging behaviours such as the shear softening effects observed in the deformation of polystyrene foam reflected by a downward concavity in stress-deformation curves, see, e.g., the work of Zhang et al. (1997; 1998), are not known to be straightforwardly modelled by the existing hyperelastic strain energy functions. Indeed, beside the *parent* model in Eq. (5) and the proposed family of models in Eq. (12), the only other model known to the authors that may be able to model this behaviour is that of Lopez-Pamies (2010). Not only were the proposed family of models in this work capable of capturing this behaviour, the models also successfully characterised the ensuing instability. To the best of our knowledge, such modelling results have not been presented elsewhere in relation to the finite deformation of compressible foams and elastomers.

An interesting direction for the future development is the incorporation of the rate-effects into modelling the mechanical behaviour of elastomers. Recently, Upadhyay et al. (2021) explored the modelling of the rate-effects in the deformation of cross-linked elastomers by adding a viscous 'dissipation' function to the hyperelastic strain energy W. Such an approach was previously considered and presented in relation to the deformation behaviour of heart valves by Anssari-Benam et al. (2017; 2018), within the context of incompressibility. Given that many compressible foams and elastomers also exhibit rate-effects (see, e.g., Zhang et al., 1997; 1998; Upadhyay et al., 2021), extending the proposed models herein to include the rate-dependent behaviour of elastomers merits further investigation.

Acknowledgments We are grateful to the reviewers for their constructive comments on an earlier version of the manuscript.

Appendix A – Tabulated experimental data

Table A1 – Experimental data on industrial and commercial polyurethane foam samples under uniaxial tension, reproduced from El-Ratal and Mallick (1996).

Industrial polyurethane foam sample			Commercial polyurethane foam sample		
λ [-]	λ_T [-]	T [kPa]	λ [-]	λ_T [-]	T [kPa]
1	1	0	1	1	0
1.14	0.96	5.51	1.10	0.97	1.79
1.22	0.95	9.45	1.19	0.92_5	5.91
1.25_5	0.93	13.77	1.25_5	0.89	10.66
1.29	0.91	18.46	1.29	0.87	15.62
1.32	0.88	24.35	1.33	0.84	21.54
1.35	0.86	31.07	1.37	0.82	27.63
1.37	0.84	37.31	1.38_5	0.80	35.62_5
1.39	0.83	43.57	1.40	0.78	43.03
1.41_5	0.81	50.85	1.42	0.76	51.04

Table A2 – Experimental data for a polyethylene foam sample under uniaxial and equi-biaxial compression reproduced from Kossa and Berezvai (2016).

Uniaxial compression			Equi-biaxial compression		
λ [-]	λ_T [-]	T [MPa]	λ [-]	λ_T [-]	T [MPa]
1	1	0	1	1	0
0.95	1.01	-9.00	0.95	1.01	-14.23
0.90	1.012	-16.89	0.90	1.02	-28.19
0.85	1.012	-25.40	0.85	1.04	-40.94
0.80	1.02	-32.29	0.80	1.05	-56.55
0.75	1.03	-39.10	0.75	1.06	-76.05
0.70	1.03_5	-46.96_5	0.70	1.07	-101.13
0.65	1.04	-56.30	0.65	1.08	-136.28
0.60	1.05	-67.20_5	0.60	1.10	-186.69
0.55	1.06	-80.09	0.55	1.11_5	-270.73
0.50	1.07	-95.64			
0.45	1.07_5	-114.60			
0.40	1.09	-138.58			
0.35	1.10	-169.81			
0.30	1.11	-212.71			
0.25	1.13	-277.80			

Table A3 – Experimental data for a polymeric foam sample under uniaxial and simple shear deformations reproduced from Yan et al. (2021).

Uniaxial compression			Simple Shear	
λ [-]	λ_T [-]	T [MPa]	γ [-]	T [MPa]
1	1	0	0	0
0.98	1.00_{04}	-0.01	0.02	0.00_5
0.96	1.00_2	-0.03	0.03	0.01
0.94	1.00_3	-0.04	0.05	0.01_4
0.92	1.00_4	-0.05	0.06	0.02
0.90	1.00_6	-0.06	0.08	0.02_3
0.88	1.00_7	-0.07_5	0.10	0.03
0.86	1.00_9	-0.09	0.11	0.03_2
0.84	1.01	-0.10	0.13	0.04
0.82	1.01_3	-0.11	0.14	0.04_1
0.80	1.01_5	-0.12	0.16	0.04_5
0.78	1.01_8	-0.13	0.18	0.05
0.76	1.02	-0.14	0.19	0.05_4
0.74	1.02_2	-0.16	0.21	0.06
0.72	1.02_5	-0.17	0.22	0.06_3
0.70	1.03	-0.18	0.24	0.07
0.68	1.03_1	-0.20	0.26	0.07_2
0.66	1.03_5	-0.21	0.27	0.08
0.64	1.04	-0.23	0.29	0.08_2
0.62	1.04_2	-0.25	0.30	0.09
0.60	1.05	-0.27	0.32	0.09_2
0.58	1.05_1	-0.31	0.34	0.10
0.56	1.06	-0.35	0.35	0.10_2
0.54	1.06_2	-0.42	0.37	0.11
0.52	1.07	-0.52	0.38	0.11_4
0.50	1.07_4	-0.69	0.40	0.12

Table A4 – Experimental data for a polystyrene foam specimen under simple shear deformation due to Zhang et al. (1998).

Simple Shear	
γ [-]	T [MPa]
0	0
0.01	0.03
0.03	0.06
0.05	0.08
0.07	0.09
0.09	0.09_5
0.11	0.10
0.13	0.09_5
0.15	0.09_4
0.17	0.09_2
0.19	0.09

Table A5 – Experimental data for a PVA gel specimen under uniaxial tension due to Urayama et al. (1993).

Uniaxial compression		
λ [-]	λ_T [-]	T [kPa]
1	1	0
1.14	0.96	0.30
1.17	0.95	0.36
1.22	0.94	0.45_5
1.27	0.92	0.54
1.36	0.90	0.61
1.42_5	0.89	0.65
1.52	0.87	0.69_5
1.74	0.83	0.78
1.95	0.80	0.91
2.12	0.77_5	1.05
2.33	0.75	1.24
2.66	0.72	1.64
3.07_5	0.68	2.22
3.35	0.66	2.59

Table A6 – Experimental data for a hydrogel specimen under uniaxial and simple shear deformations due to Upadhyay et al. (2020).

Uniaxial compression			Simple Shear	
λ [-]	λ_T [-]	T [kPa]	γ [-]	T [kPa]
0.80	1.11	-135.85	0	0
0.85	1.08	-94.95	0.00_7	1.34
0.87_5	1.06	-74.97	0.01	2.93
0.90	1.05	-57.05	0.02_5	6.10
0.95	1.02	-26.04	0.04	8.78
1.00	1.00	0	0.05	11.46
1.01	0.99_5	8.91	0.06	13.90
1.02	0.99	17.45	0.07	16.22
1.04	0.98	34.97	0.08_5	19.02
1.05	0.98	43.69	0.10	21.95
1.06	0.97	52.83	0.11	24.63

Table A7 – Experimental data for an alginate-polyacrylamide hydrogel sample undergoing uniaxial deformation, due to Sun et al. (2012).

Uniaxial compression		
λ [-]	λ_T [-]	T [MPa]
1.00	1.00	0
3.00	0.61	0.17
5.00	0.48	0.37
7.00	0.42	0.56
9.00	0.37	0.76_5
11.00	0.34	0.99
13.00	0.31_5	1.24
15.00	0.29_5	1.49
17.00	0.28	1.79
19.00	0.26_5	2.08
21.00	0.25	2.37
23.00	0.24	2.65

References

Anssari-Benam, A., 2021. On a new class of non-Gaussian molecular based constitutive models with limiting chain extensibility for incompressible rubber-like materials. Math. Mech. Solids 26, 1660-1674. (https://doi.org/10.1177/10812865211001094)

Anssari-Benam, A., Bucchi, A., 2018. Modelling the deformation of the elastin network in the aortic valve. J. Biomech. Eng. 140, 011004. (https://doi.org/10.1115/1.4037916)

Anssari-Benam, A., Bucchi, A., 2021. A generalised neo-Hookean strain energy function for application to the finite deformation of elastomers. Int. J. Non. Linear Mech. 128, 103626. (https://doi.org/10.1016/j.ijnonlinmec.2020.103626)

Anssari-Benam, A., Bucchi, A., Horgan, C.O., Saccomandi, G., 2021a. Assessment of a new isotropic hyperelastic constitutive model for a range of rubber-like materials and deformations, Rubber Chem. Technol. (https://doi.org/10.5254/rct.21.78975)

Anssari-Benam, A., Bucchi, A., Saccomandi, G., 2021b. Modelling the inflation and elastic instabilities of rubber-like spherical and cylindrical shells using a new generalised neo-Hookean strain energy function. J. Elast. (https://doi.org/10.1007/s10659-021-09823-x)

Anssari-Benam, A., Bucchi, A., Saccomandi, G., 2021c. On the central role of the invariant I_2 in nonlinear elasticity. Int. J. Eng. Sci. 163, 103486. (https://doi.org/10.1016/j.ijengsci.2021.103486)

Anssari-Benam, A., Bucchi, A., Screen, H.R.C., Evans, S.L., 2017. A transverse isotropic viscoelastic constitutive model for aortic valve tissue. R. Soc. Open Sci. 4, 160585. (https://doi.org/10.1098/rsos.160585)

Anssari-Benam, A., Horgan, C.O., 2021. On modelling simple shear for isotropic incompressible rubber-like materials. J. Elast. 147, 83-111. (https://doi.org/10.1007/s10659-021-09869-x)

Anssari-Benam, A., Horgan, C.O., 2022a. Extension and torsion of rubber-like hollow and solid circular cylinders for incompressible isotropic hyperelastic materials with limiting chain extensibility. Eur. J. Mech. A Solids 92, 104443. (https://doi.org/10.1016/j.euromechsol.2021.104443)

Anssari-Benam, A., Horgan, C.O., 2022b. A three-parameter structurally motivated robust constitutive model for isotropic incompressible unfilled and filled rubber-like materials. Eur. J. Mech. A Solids 95, 104605. (https://doi.org/10.1016/j.euromechsol.2022.104605)

Anssari-Benam, A., Tseng, Y.-T., Bucchi, A., 2018. A transverse isotropic constitutive model for the aortic valve tissue incorporating rate-dependency and fibre dispersion: application to biaxial deformation. J. Mech. Behav. Biomed. Mater. 85, 80-93. (https://doi.org/10.1016/j.jmbbm.2018.05.035)

Beatty, M.F., Stalnaker, D.O., 1986. The Poisson function of finite elasticity. J. Appl. Mech. 53, 807-813. (https://doi.org/10.1115/1.3171862)

Bischoff, J.E., Arruda, E.M., Grosh, K., 2001. A new constitutive model for the compressibility of elastomers at finite deformations. Rubber Chem. Technol. 74, 541-559. (https://doi.org/10.5254/1.3544956)

Blatz, P.J., Ko, W.L., 1962. Application of finite elastic theory to the deformation of rubbery materials. Trans. Soc. Rheol. 66, 223-251. (https://doi.org/10.1122/1.548937)

Cai, S., Hu, Y., Zhao, X., Suo, Z., 2010. Poroelasticity of a covalently crosslinked alginate hydrogel under compression. J. Appl. Phys. 108, 113514. (https://doi.org/10.1063/1.3517146)

Davidson, J.D., Goulbourne, N.C., 2013. A nonaffine network model for elastomers undergoing finite deformations. J. Mech. Phys. Solids 61, 1784-1797. (https://doi.org/10.1016/j.jmps.2013.03.009)

Destrade, M., Saccomandi, G., Sgura, I., 2017. Methodical fitting for mathematical models of rubber-like materials. Proc. R. Soc. A 473, 20160811. (http://doi.org/10.1098/rspa.2016.0811)

Ding, F., Liu, T., Zhang, H., Liu, L., Li, Y., 2021. Stress-strain curves for polyurethane elastomers: A statistical assessment of constitutive models. J. Appl. Polym. Sci. 138, e51269. (https://doi.org/10.1002/app.51269)

El-Ratal, W.H., Mallick, P.K., 1996. Elastic response of flexible polyurethane foams in uniaxial tension. J. Eng. Mater. Technol. 118, 157-161. (https://doi.org/10.1115/1.2804881)

Flory, P.J., 1961. Thermodynamic relations for high elastic materials. Trans. Faraday Soc. 57, 829-838. (https://doi.org/10.1039/TF9615700829)

Gent, A.N., 1996. A new constitutive relation for rubber. Rubber Chem. Technol. 69, 59-61. (https://doi.org/10.5254/1.3538357)

Gent, A.N., Lindley, P.B., 1959. Internal rupture of bonded rubber cylinders in tension. Proc. R. Soc. Lond. A 249, 195-205. (https://doi.org/10.1098/rspa.1959.0016)

Gent, A.N., Thomas, A.G., 1958. Forms for the stored (strain) energy function for vulcanized rubber. J. Polym. Sci. 28, 625-628. (https://doi.org/10.1002/pol.1958.1202811814)

Gültekin, O., Dal, H., Holzapfel, G.A., 2019. On the quasi-incompressible finite element analysis of anisotropic hyperelastic materials. Comput. Mech. 63, 443-453. (https://doi.org/10.1007/s00466-018-1602-9)

Hill R., 1979. Aspects of invariance in solid mechanics. Adv. Appl. Mech. 18, 1-75. (https://doi.org/10.1016/S0065-2156(08)70264-3)

Holt, W.L., McPherson, A.T., 1936. Change of volume for rubber on stretching: Effects of time, elongation, and temperature. J. Res. Nat. Bur. Stand. 17, 657-678. (https://doi.org/10.5254/1.3538995)

Horgan, C.O., 2021. A note on a class of generalized neo-Hookean models for isotropic incompressible hyperelastic materials. Int. J. Non-Linear Mech. 129, 103665. (https://doi.org/10.1016/j.ijnonlinmec.2020.103665)

Horgan, C.O., Murphy, J.G., 2007a. Constitutive models for almost incompressible isotropic elastic rubber-like materials. J. Elast. 87, 133-146. (https://doi.org/10.1007/s10659-007-9100-x)

Horgan, C.O., Murphy, J.G., 2007b. The effects of compressibility on inhomogeneous deformations for a class of almost incompressible isotropic nonlinearly elastic materials. J. Elast. 88, 207-221. (https://doi.org/10.1007/s10659-007-9131-3)

Horgan, C.O., Murphy, J.G., 2009a. Constitutive modeling for moderate deformations of slightly compressible rubber. J. Rheol. 53, 153-168. (https://doi.org/10.1122/1.3037263)

Horgan, C.O., Murphy, J.G., 2009b. On the volumetric part of strain-energy functions used in the constitutive modeling of slightly compressible solid rubbers. Int. J. Solids Struct. 46, 3078-3085. (https://doi.org/10.1016/j.ijsolstr.2009.04.007)

Horgan, C.O., Murphy, J.G., 2009c. A generalization of Hencky's strain-energy density to model the large deformations of slightly compressible solid rubbers. Mech. Mater. 41, 943-950. (https://doi.org/10.1016/j.mechmat.2009.03.001)

Horgan, C.O., Murphy, J.G., 2009d. Compression tests and constitutive models for the slight compressibility of elastic rubber-like materials. Int. J. Eng. Science 47, 1232-1239. (https://doi.org/10.1016/j.ijengsci.2008.10.009)

Horgan, C.O., Murphy, J.G., 2010. Simple shearing of incompressible and slightly compressible isotropic nonlinearly elastic materials. J. Elast. 98, 205-221. (https://doi.org/10.1007/s10659-009-9225-1)

Horgan, C.O., Saccomandi, G., 2004. Constitutive models for compressible nonlinearly elastic materials with limiting chain extensibility. J. Elast. 77, 123-138. (https://doi.org/10.1007/s10659-005-4408-x)

Kossa, A., Berezvai, S., 2016. Novel strategy for the hyperelastic parameter fitting procedure of polymer foam materials. Polym. Test. 53, 149-155. (http://dx.doi.org/10.1016/j.polymertesting.2016.05.014)

Li, K., Holzapfel, G.A., 2019. Multiscale modeling of fiber recruitment and damage with a discrete fiber dispersion method. J. Mech. Phys. Solids 126, 226-244. (https://doi.org/10.1016/j.jmps.2019.01.022)

Li, K., Ogden, R.W., Holzapfel, G.A., 2018. Modeling fibrous biological tissues with a general invariant that excludes compressed fibers, J. Mech. Phys. Solids 110, 38-53. (https://doi.org/10.1016/j.jmps.2017.09.005)

Lopez-Pamies, O., 2010. A new I_1-based hyperelastic model for rubber elastic materials. C. R. Mecanique 338, 3-11. (https://doi.org/10.1016/j.crme.2009.12.007)

Normand, V., Lootens, D.L., Amici, E., Plucknett, K.P., Aymard, P., 2000. New insight into agarose gel mechanical properties. Biomacromolecules 1, 730-738. (https://doi.org/10.1021/bm005583j)

Ogden, R.W., 1972. Large deformation isotropic elasticity: on the correlation of theory and experiment for compressible rubberlike solids. Proc. R. Soc. Lond. A 328, 567-583. (http://doi.org/10.1098/rspa.1972.0096)

Ogden, R.W., 1976. Volume changes associated with the deformation of rubber-like solids. J. Mech. Phys. Solids 24, 323-338. (https://doi.org/10.1016/0022-5096(76)90007-7)

Ogden, R.W., Saccomandi, G., Sgura, I., 2004. Fitting hyperelastic models to experimental data. Comput. Mech. 34, 484-502. (https://doi.org/10.1007/s00466-004-0593-y)

Peng, S.T.J., Landel, R.F., 1975. Stored energy function and compressibility of compressible rubberlike materials under large strain. J. Appl. Phys. 46, 2599-2604. (http://dx.doi.org/10.1063/1.321936)

Penn, R.W., 1970. Volume changes accompanying the extension of rubber. Trans. Soc. Rheol. 14, 509-517. (http://dx.doi.org/10.1122/1.549176)

Pucci, E., Saccomandi, G., 2002. A note on the Gent model for rubber-like materials. Rubber Chem. Technol. 75, 839-852. (https://doi.org/10.5254/1.3547687)

Simo, J.C., Taylor, R.L., 1982. Penalty function formulations for incompressible nonlinear elastostatics. Comput. Methods Appl. Mech. Eng. 35, 107-118. (https://doi.org/10.1016/0045-7825(82)90035-4)

Sun, J.-Y., Zhao, X., Illeperuma, W.R.K., Chaudhuri, O., Oh, K.H., Mooney, D.J., Vlassak, J.J., Suo, Z., 2012. Highly stretchable and tough hydrogels. Nature 489, 133-136. (https://doi.org/10.1038/nature11409)

Sussman, T., Bathe, K.J., 1987. A finite element formulation for nonlinear incompressible hyperelastic and inelastic analysis. Comput. Struct. 26, 357-409. (https://doi.org/10.1016/0045-7949(87)90265-3)

Taylor, R.L., 2013. FEAP – A Finite Element Analysis Program, Version 8.4 User Manual, University of California at Berkeley. Berkeley, California.

Upadhyay, K., Subhash, G., Spearot, D., 2020. Hyperelastic constitutive modeling of hydrogels based on primary deformation modes and validation under 3D stress states. Int. J. Eng. Sci. 154, 103314. (https://doi.org/10.1016/j.ijengsci.2020.103314)

Upadhyay, K., Spearot, D., Subhash, G., 2021. Validated tensile characterization of the strain rate dependence in soft materials. Int. J. Impact Eng. 156, 103949. (https://doi.org/10.1016/j.ijimpeng.2021.103949)

Urayama, K., Takigawa, T., Masuda, T., 1993. Poisson's ratio of poly(vinyl alcohol) gels. Macromolecules 26, 3092-3096. (https://doi.org/10.1021/ma00064a016)

Valanis, K.C., Landel, R.F., 1967. The strain-energy function of a hyperelastic material in terms of the extension ratios. J. appl. Phys. 38, 2997-3002. (https://doi.org/10.1063/1.1710039)

Yan, S., Jia, D., Yu, Y., Wang, L., Qiu, Y., Wan, Q., 2021. Novel strategies for parameter fitting procedure of the Ogden hyperfoam model under shear condition. Eur. J. Mech. A Solids 86, 104154. (https://doi.org/10.1016/j.euromechsol.2020.104154)

Yeoh, O.H., 1997. Hyperelastic material models for finite element analysis of rubber. J. nat. Rubb. Res. 12, 142-153.

Zhang, J., Lin, Z., Wong, A., Kikuchi, N., Li, V.C., Yee, A.F., Nusholtz, G.S., 1997. Constitutive modeling and material characterization of polymeric foams. J. Eng. Mater. Technol. 119, 284-291. (https://doi.org/10.1115/1.2812258)

Zhang, J., Kikuchi, N., Li, V., Yee, A., Nusholtz, G., 1998. Constitutive modeling of polymeric foam material subjected to dynamic crash loading. Int. J. Impact Engn. 21, 369-386. (https://doi.org/10.1016/S0734-743X(97)00087-0)